

# Rounded Rear Pyramidal Texture for High Efficiency Silicon Solar Cells

Ngwe Zin<sup>1</sup>, Keith McIntosh<sup>2</sup>, Teng Kho<sup>1</sup>, Evan Franklin<sup>1</sup>, Kean Fong<sup>1</sup>, Matthew Stocks<sup>1</sup>, Er-Chien Wang<sup>1</sup>, Tom Ratcliff<sup>1</sup> and Andrew Blakers<sup>1</sup>

<sup>1</sup>Australian National University, Canberra, ACT, 2601, Australia

<sup>2</sup>PV Lighthouse, Coledale, NSW 2515, Australia

**Abstract** — Interdigitated back-contact (IBC) solar cells developed in the past two years have efficiencies in the range 24.4%–25.6%. As high as these efficiencies are, there are opportunities to increase them further by improving on the light trapping. Silicon solar cells incorporating double-sided pyramidal texture are capable of superior light trapping than cells with texture on just the front. One of the principle losses of double-sided pyramidal texture is the light that escapes after a second pass through the cell when the facet angles are the same on the front and rear. This contribution investigates how this loss might be reduced by changing the facet angle of the rear pyramids. A textured pyramid rounding is introduced to improve the light trapping. The reduction in surface recombination that rounding the facets introduces is also evaluated. With confocal microscopy, spectrophotometry and ray tracing, the rounding etch time required to yield the best light trapping is investigated. With photoconductance lifetime measurements, the surface recombination is found to continue to decrease as the rounding time increases. The spectrophotometry and ray tracing suggests that the double sided textured samples featuring rounded rear pyramids have superior light trapping to the sample with a planar rear surface. The high-efficiency potential of rounded textured pyramids in silicon solar cells is demonstrated by the fabrication of 24% efficient back-contact silicon solar cells.

**Index Terms** — double-sided texture, rear texture, isotropic acid texture, light trapping, diffusions, passivation, PECVD nitride, ALD AlO<sub>x</sub>, back-contact, ray trace, solar cell, high efficiency, polyimide, back contact, IBC, PERL.

## 1. Background

The light trapping in most high efficiency silicon solar cell designs involves a textured front surface and a planar rear surface [1-7]. The light trapping in these cells is less than ideal because a significant fraction of light rays incident to the rear surface are reflected into the escape cone of a front pyramid and are coupled out [8]. Modifying the rear surface, such as by creating a Lambertian reflector, redirects the first-pass light to avoid this optical path and therefore increases the photogeneration current, as in Figure 1.

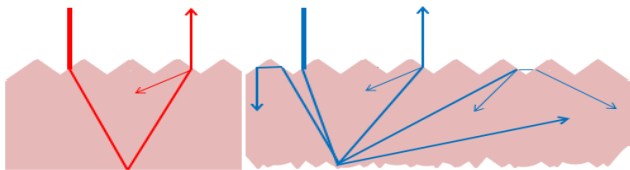


Figure 1: Comparison of rays when the rear surface is specular (red) and Lambertian (blue). Many rays reflected at obtuse angles

by the Lambertian surface are internally reflected by the front texture by total internal reflection [9].

Numerous light trapping schemes have been investigated to improve solar cell efficiency. These include the tiler's pattern [8], perpendicular grooves [8], honeycomb texture realized by isotropic etching [10], plasmonic nanoparticles on the rear of wafer-based silicon solar cell structure [11], simple prism pyramidal texture realized by mechanical grooving [12], pigmented rear reflector [13], dielectric back scattering [14] and random pyramidal texture via alkaline etch solution [15]. Of these, the last scheme is the most widely-used and well-established method in the fabrication of silicon solar cells.

The application of random pyramidal double-sided texture (DST) on the front and rear of silicon solar cells has been shown to provide superior light trapping properties relative to silicon solar cells with front texture and rear planar morphologies, as it helps to randomize the direction of light absorbed and at the same time reduces the chance of escape [8]. However, in DST silicon solar cells, the benefit of superior light trapping could be at least partially offset by the increase in carrier recombination due to increased surface area, sharp peaks and troughs, and in the case of SiO<sub>2</sub> passivation, an exposure of crystal orientation <111>, which is well known for introducing a high density of dangling bonds [16]. Moreover, thermal SiO<sub>2</sub> on textured surfaces has been concluded to increase bulk recombination due to volume expansion associated with the thermal SiO<sub>2</sub> generating compressive and tensile stresses at the peaks and troughs of textured pyramids [17]. A stack of thermal oxide and low pressure chemical vapour deposited (LPCVD) silicon nitride (Si<sub>3</sub>N<sub>4</sub>), which has been shown to provide both very good passivation and electrical isolation required for high-efficiency back-contact cells [18], also increases the surface recombination significantly on the random pyramidal textured surfaces [4]. Passivation layers such as aluminum oxide (AlO<sub>x</sub>) [19-21] and silicon nitride (SiN<sub>x</sub>) [22] provide outstanding passivation on planar and textured pyramidal surfaces. However, these films are typically imperfect owing to pinhole formation during deposition [23] and therefore do not provide adequate isolation between metal and silicon substrate. This can lead to poor shunt resistance and increased recombination, both of which are major obstacles in the development of high efficiency silicon solar cells [24, 25].

To overcome the aforementioned limitations with conventional pyramidal textured rear surfaces, this paper proposes rounding the sharp textured tips to reduce the likelihood of shunting and to reduce surface recombination, while maintaining or even enhancing the light trapping benefit of textured rear surface. Heng *et al.* found that the application of truncated textured pyramids, as compared to fully textured pyramids, resulted in an increased open circuit voltage of 15 mV in their development of high efficiency silicon solar cells [26].

In this contribution, we investigate DST incorporating rounded rear pyramids to increase light trapping while maintaining comparatively low surface recombination. The rounding etch is performed with an HF:HNO<sub>3</sub> acid mixture. Surface recombination after various degrees of rounding is investigated after depositing a PECVD SiN<sub>x</sub> passivating film. The effectiveness of light trapping is evaluated by spectrophotometry and ray tracing. Solar cells incorporating double-sided texture with rounded rear pyramids were fabricated for the first time to our knowledge to assess the fabrication feasibility of back-contact silicon solar cells incorporating rounded textured pyramids.

## 2. Rounded Pyramid Sample Preparations

In order to simultaneously evaluate the surface recombination properties and light-trapping enhancement potential of different pyramid rounding regimes, two sets of substrate types are prepared. These sample types are illustrated in Figure 2, and a detailed description of sample preparation given below.

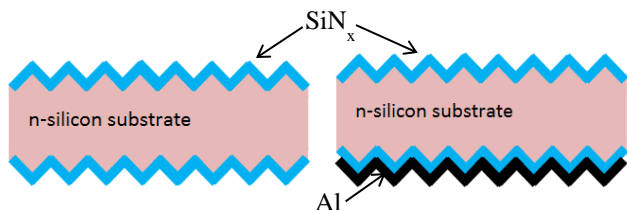


Figure 2: For the recombination study (left), samples have double-sided planar, texture or rounded texture. For light trapping investigation (right), samples have identical front side pyramidal texture with planar, texture or rounded texture at the rear.

Recombination analysis samples were fabricated using high resistivity (>100 Ω.cm) n-type <100> 400 μm thick silicon wafers, which were first saw-damage etched in Tetramethylammonium hydroxide (TMAH) at 85°C for 10 minutes. Symmetric random pyramid textured samples were subsequently created by texture etching in a 4% TMAH solution containing isopropyl alcohol (IPA) and some silicon seed crystals obtained from 25% TMAH solution precipitates, at 85°C for 60 minutes. Samples were then subjected to the ‘rounding etch’, an acid solution of 1:10 HF: HNO<sub>3</sub> at room temperature. An HF:HNO<sub>3</sub> solution etches silicon isotropically, which results in the sharp peaks, ridges and troughs of pyramids becoming rounded, a reduction in the height of pyramids and a subsequent shallowing of the pyramid facet angle. The rounding etch

duration was varied between samples, resulting in differing degrees of rounding and differing pyramid heights. These samples and associated measurement results are referred to throughout as ‘No R\_Etch’ (no rounding etch), ‘Short R\_Etch’ (30 seconds rounding etch), ‘Medium R\_Etch’ (60 seconds rounding etch), and ‘Long R\_Etch’ (90 seconds rounding etch). An additional wafer which received no texturing or rounding etch is used as a reference sample, and is referred to as the ‘Planar R’ sample.

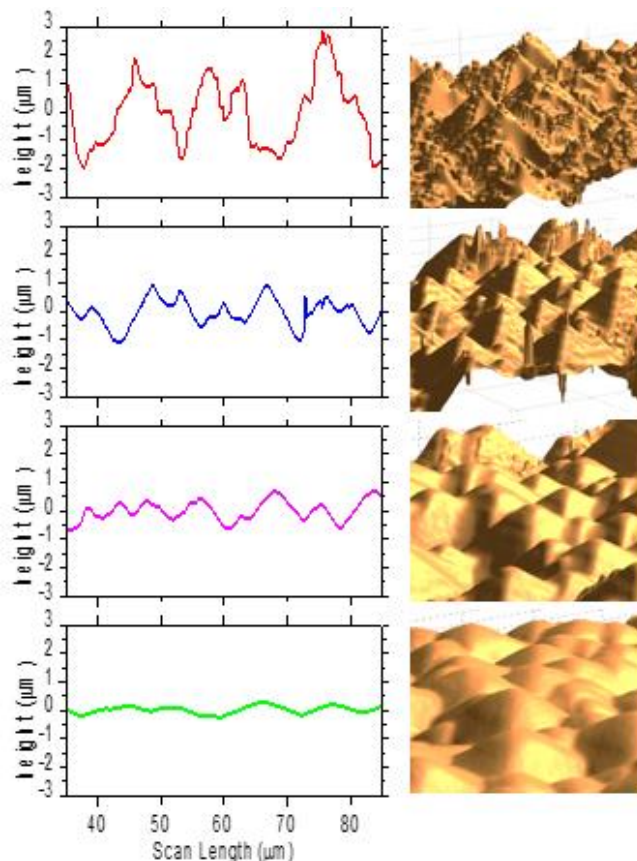


Figure 3: 2D surface profile and 3D images of textured pyramids scanned by the confocal microscope. Textured pyramids have approximately 3.6μm (top), 2μm, 1.5μm and 1μm (bottom) in height for 0s, 30s, 60s and 90s of etching in HF:HNO<sub>3</sub>.

Confocal microscopy was then used to generate 2D surface profile and 3D images of the rounded pyramids to analyze different pyramid heights and planarization. The confocal microscopy is an optical imaging technique that increases optical resolution and contrast of a micrograph by means of adding a spatial pinhole placed at the confocal plane of the lens to eliminate out-of-focus light, thus enabling the reconstruction of three-dimensional structures from the obtained images [27]. Figure 3 shows 2D surface profile and 3D images of the rounded pyramids with different heights and morphologies. Varying the etch time of HF:HNO<sub>3</sub> results in textured pyramids with 3.6 μm (as textured), 2 μm, 1.5 μm and 1 μm in height approximately for No R\_Etch, Short R\_Etch, Medium R\_Etch and Long R\_Etch, respectively. As shown in Figure 3, increasing the etch time

not only reduces the pyramid size but also smoothens the pyramid peaks and troughs.

Samples for the analysis of light trapping were then prepared by saw damage etching the high resistivity ( $>100 \Omega/\square$ ) n-type  $\langle 100 \rangle$  silicon samples in TMAH at  $85^\circ\text{C}$  for 10 minutes. Following the damage etch, all samples underwent random pyramidal texturing at  $85^\circ\text{C}$  for 60 minutes. Following the texture, the front side of textured samples was masked with a polymer [28] having a thickness of  $7 \mu\text{m}$  and processed to give a rounding etch on the rear surface in the isotropic acid mixture for 0s, 30s, 60s, 90s and 180s, respectively, to aim for rear pyramid heights with  $3.6 \mu\text{m}$ ,  $2 \mu\text{m}$ ,  $1.5 \mu\text{m}$ ,  $1 \mu\text{m}$  and smooth planar morphology. The polymer was then removed from the samples and  $\text{SiN}_x$  ( $\sim 70 \text{ nm}$ ) was deposited on both sides of all samples. Aluminum ( $\sim 1 \mu\text{m}$ ) was also deposited on the rear of the samples to create a back reflector. The samples have a final thickness of  $\sim 370 \mu\text{m}$ . These samples therefore mimic a solar cell device. Table 1 illustrates samples with different front and rear surface conditions for recombination and light trapping studies.

Table 1: Samples for recombination and light trapping studies with different front and rear surface conditions. Tex stands for 60 min of texture in TMAH, while R represents rounding etch (in seconds) in the  $\text{HF:HNO}_3$  solution.

	Recombination		Light Trapping	
	Front	Rear	Front	Rear
Planar	Planar	Planar		
Planar Rear			Tex	Planar
No R_Etch	Tex+0s R	Tex+0s R	Tex	Tex+0s R
Short R_Etch	Tex + 30s R	Tex + 30s R	Tex	Tex + 30s R
Medium R_Etch	Tex + 60s R	Tex + 60s R	Tex	Tex + 60s R
Long R_Etch	Tex + 90s R	Tex + 90s R	Tex	Tex + 90s R

### 3. Recombination at Rounded Pyramidal Textured Surfaces

The recombination current prefactor  $J_0$  was measured by photoconductance decay using the Kane and Swanson technique [29] assuming an intrinsic carrier concentration of  $n_i = 8.95 \times 10^9 \text{ cm}^{-3}$  (at  $25^\circ\text{C}$ ). Figure 4 shows  $J_0$  of planar and textured samples. Of all samples, the No R\_Etch (i.e. 0s rounding etch) sample has the largest  $J_0$  (per side) of  $15 \text{ fA/cm}^2$ ; this is expected since it has the largest surface area and the sharpest peaks and valleys as compared to other samples (see Figure 3). The  $J_0$  is significantly reduced by etching  $1.6 \mu\text{m}$  of silicon (i.e. down to  $\sim 5 \text{ fA/cm}^2$ , which is only  $2 \text{ fA/cm}^2$  higher than the planar sample). Thereafter, the  $J_0$  reduces only slightly at a  $\sim 0.5 \text{ fA/cm}^2$  for each half-micron of Si etched. Further etching of the sample in  $\text{HF:HNO}_3$  removes the pyramids and planarizes the surface.

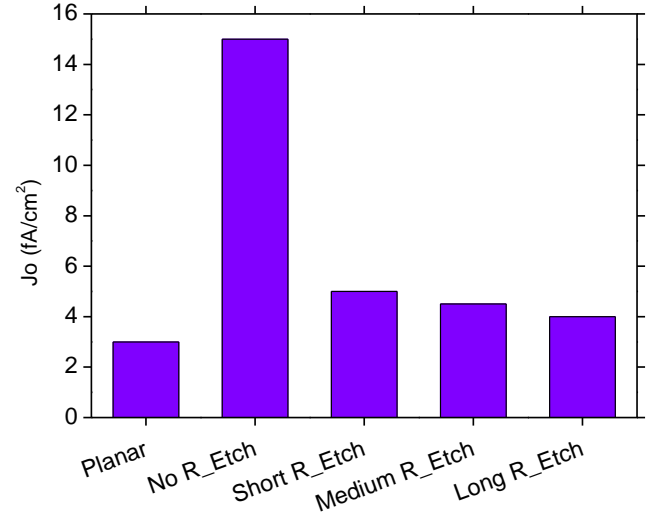


Figure 4:  $J_0$  of samples whose front and rear surfaces are (i) planar, (ii) textured with No R\_Etch, Short R\_Etch, Medium R\_Etch and Long R\_Etch.

### 4. Light Trapping in Rounded Textured Pyramids

The optical behavior of the samples was next assessed by spectrophotometry. Figure 5 plots the measured total absorption against wavelength for each sample. It is difficult to conclude much from these results because we cannot distinguish between absorption in the silicon and absorption in the rear Al (i.e. parasitic absorption). It is evident, however, that there is a substantial difference in behavior between the samples, emphasizing that the variations in rear rounding have a significant impact on optical behavior. The large disparity between the non-rounded sample (red symbols, No R\_Etch) and the remaining samples is unexpected and may in fact be systematic error. Investigations into the optical behavior continues, including the application of photoluminescent spectroscopy.

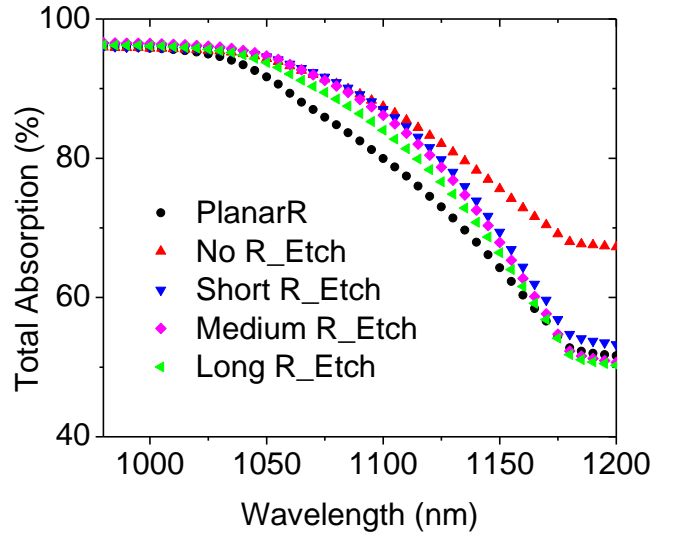


Figure 5: Total absorption 1-R-T of samples with different front and rear surface conditions measured by the spectrometry technique. Measured T is effectively zero on samples with Al (1  $\mu\text{m}$ ) at the rear. Apart from the control that has planar morphology on both front and rear, The samples have identical front texture but differing rear texture.

The optical behavior was also assessed with a wafer ray tracer [31]. Inputs to these simulations, including the substrate and dielectric thickness, are listed in Table 2. Most relevant to this study is, of course, how the rear surface is treated. It is difficult to approximate the etched pyramids of Figure 3 because of the rounding at the peaks and troughs. Nevertheless, we make the approximation in the ray tracing that there is no rounding, and that only the pyramid height (and hence pyramid base angle) changes. That is, we assume the pyramids width is 5  $\mu\text{m}$  for all cases, and we set the height of the pyramids to be 3.5, 2, 1.5, 1, 0.5 and 0  $\mu\text{m}$ , which corresponds to facet angles of 54.7, 38.7, 31.0, 21.8, 11.3 and 0 $^\circ$  to represent the various degrees in rounding. The selected pyramid heights are approximately those observed for the samples—see Figure 3.

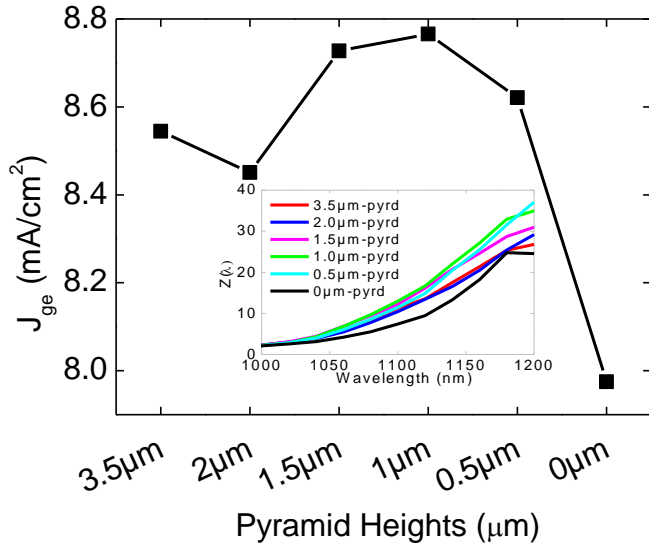


Figure 6:  $J_{gen}$  simulated for the wavelength of 950-1200 nm by the wafer ray tracer. The pathlength enhancement  $Z$  is shown in the inset figure.

Figure 6 plots the results of the ray tracing in terms of (i) the current density generated in the silicon  $J_{gen}$  over the range 950–1200 nm, and (ii) optical pathlength enhancement  $Z(\lambda)$ . The ray tracing suggests that there should be an optimal rear pyramid angle. With 54.7 $^\circ$  on the front and rear surface, many rays are coupled out of the cell in the first pass, and with a planar rear surface, many rays are coupled out of the cell after the second pass. An angle between 0 and 54.7 $^\circ$  leads to superior light trapping.

Thus, we experimentally observe that recombination at the rear surface is dramatically reduced, from 15  $\text{fA}/\text{cm}^2$  to  $\sim 3\text{fA}/\text{cm}^2$  by a short rounding etch. And from ray tracing, we

expect there to be an optimal rounding time that maximizes light trapping, but this has neither been confirmed nor contradicted by optical experiments.

## 5. Cells Development and Discussion

Back-contact silicon solar cells featuring rear rounded textured pyramids were developed to assess the feasibility of integrating rounded texture in the cells fabrication process.

Samples with rear planar and rounded pyramidal textured conditions were used. A single rounding condition with the etch duration of 60s was adopted in this evaluation. Cells were fabricated from high resistivity  $\langle 100 \rangle$  FZ wafers. The development process, device structure and process parameters of back contact silicon solar cells in this contribution is based on the publication elsewhere [18]. Cells with planar and rounded pyramidal texture conditions have the final thickness of 230  $\mu\text{m}$  and 170  $\mu\text{m}$  thickness, respectively.

Table 3 shows the current-voltage (JV) of the cells measured under one-sun illuminated condition using in-house solar simulator. However, we have recently discovered that the in-house solar simulator used in this measurement introduces spectral mismatch to our cells in the long wavelength (i.e.  $> 1000$  nm), which could have possibly led to the significant underestimate of the light trapping enhancement. A discussion of this will be made in the later publications.

Efficiencies in the range 23.6–24.4% are attained. Relative to the cell with rear planar, the cell with rounded rear pyramids have achieved an increased  $J_{sc}$  of 0.25  $\text{mA}/\text{cm}^2$  (from an average of three rear-rounded textured cells compared to that of rear planar cells), despite the cell substrate being thinner by at least 60  $\mu\text{m}$ . However, a small reduction in  $V_{oc}$  is observed, as expected. Besides, the champion cell with rounded rear pyramids also suffers some fill factor (FF) loss of 0.5% (see table 3), relative to the cell with planar rear, possibly due to unknown non-ideal recombination since the pseudo FF in the DST cells with rounded pyramids is lower than that in the cell with planar rear.

As the cells with rounded rear pyramids have thinner substrates (i.e. 60 $\mu\text{m}$ ), to further analyze the performance of  $J_{sc}$  based on the increased substrate thickness, the front surface reflectance of the champion cell (frontRtex3) was first measured by the spectrophotometry. Then using  $Z(\lambda)$  simulated by the wafer ray tracer for a range of thicknesses, frontRtex3 and silicon absorption coefficient, the maximum possible  $J_{sc}$  ( $J_{sc,max}$ ) was simulated (assuming a unity collection efficiency) for a range of cell thicknesses. A similar discussion of simulating  $J_{sc,max}$  is published elsewhere [32]. The simulation indicates that the measured  $J_{sc}$  could be increased by an additional  $\sim 0.3$   $\text{mA}/\text{cm}^2$  (950-1200 nm), when the champion cell's substrate thickness is



increased to 230  $\mu\text{m}$ . Further increase in the efficiency of the DST cell with rounded rear pyramids is well within reach following the improvement in the optic and FF.

## 6. Conclusion

In conclusion, we demonstrated the increase in light trapping via double-sided texture incorporating rounded rear texture, while maintaining comparatively low surface recombination. Increasing rounding etch time makes textured pyramids smaller and smoother surface condition; resulting in improved surface passivation. Rounding the textured pyramids reduces  $J_o$  by as much as 65% relative to the  $J_o$  of fully textured pyramids (i.e. 0s rounding etch). Ray tracing suggested that optimal light trapping would arise from partially rounded rear pyramids.  $J_{sc}$  of rounded textured cells relative to that of planar rear cell is increased by 0.25  $\text{mA}/\text{cm}^2$ . 24% efficient back-contact silicon solar cell fabricated in this contribution also demonstrates the feasibility (i.e. high shunt resistance and process compatibility) of incorporating rounded texturing in the high efficiency cell developments.

## ACKNOWLEDGEMENTS

The funding of this research is supported by the Australian Solar Institute (now known as Australian Government

through the Australian Renewable Energy Agency, ARENA) through research grants of 4-F002 and RND009. The authors thank D. Macdonald for the useful discussions. This research is partially funded by Trina Solar. Responsibility for the views, information or advice expressed herein is not accepted by the Australian Government.

## APPENDIX

Table 2: Parameters used in the ray trace. 54.74°, 40°, 30°, 20°, 10° and planar are used in the X, while 2.1 $\mu\text{m}$ , 1.44 $\mu\text{m}$ , 0.91 $\mu\text{m}$ , 0.44 $\mu\text{m}$  and planar for X'.

Spectrum		AM1.5G			
	Morphology	Angle (°)	Height ( $\mu\text{m}$ )	Width ( $\mu\text{m}$ )	
Front	upright	54.74	3.54	5	
Rear	upright	X	X'	5	
	Material	Thickness (nm)			
Front film	SiO <sub>2</sub>	90			
Front film	SiN <sub>x</sub>	60			
Substrate	Si	370			
Rear film	SiN <sub>x</sub>	60			
Rear film	SiO <sub>2</sub>	1200			
Rear film	Al	1000			
Wavelength (min)	300 nm				
Wavelength (max)	1200 nm				

Table 3: Electrical parameters of back-contact cells incorporating rear rounded pyramids and planar surface.

	Area (cm <sup>2</sup> )	Voc (V)	Jsc (mA/cm <sup>2</sup> )	FF	Vmpp (mV)	Jmpp (mA/cm <sup>2</sup> )	Efficiency (%)	pFF	FFo	Rshunt Ohm-cm <sup>2</sup>	Rseries at MPP (Ohm-cm <sup>2</sup> )
RText (best)	2x2	0.705	42.05	0.811	0.609	39.36	24.04	0.823	0.847	11980	0.205
Planar (best)	2x2	0.710	41.94	0.816	0.616	39.48	24.30	0.833	0.848	24401	0.305
<b>RText (average)</b>	<b>2x2</b>	<b>0.704</b>	<b>42.050</b>	<b>0.799</b>	<b>0.608</b>	<b>38.838</b>	<b>23.602</b>	<b>0.811</b>	<b>0.847</b>	8815	0.224
<b>Planar (average)</b>	<b>2x2</b>	<b>0.709</b>	<b>41.804</b>	<b>0.812</b>	<b>0.614</b>	<b>39.214</b>	<b>23.976</b>	<b>0.828</b>	<b>0.847</b>	12234	0.306

## REFERENCES

- [1] J. Nakamura, N. Asano, T. Hieda, C. Okamoto, T. Ohnishi, M. Kobayashi, *et al.*, "Development of Heterojunction Back Contact Si Solar Cells," in *40th IEEE Photovoltaics Specialist Conference*, Denver, Colorado, 2014.
- [2] K. Masuko, M. Shigematsu, T. Hashiguchi, D. Fujishima, M. Kai, N. Yoshimura, *et al.*, "Achievement of more than 25% conversion efficiency with crystalline silicon heterojunction solar cell," in *40th IEEE PVSC*, Colorado, Denver, 2014.
- [3] N. Zin, A. Blakers, K. R. McIntosh, E. Franklin, T. Kho, K. Chern, *et al.*, "Continued Development of All-Back-Contact Silicon Wafer Solar Cells at ANU," *Energy Procedia*, vol. 33, pp. 50-63, // 2013.
- [4] N. Zin, A. Blakers, E. Franklin, T. Kho, K. McIntosh, J. Wong, *et al.*, "Progress in the Development of All-Back-Contacted Silicon Solar Cells," *Energy Procedia*, vol. 25, pp. 1-9, // 2012.
- [5] J. Zhao. (2011) Passivated Emitter Rear Locally Diffused Solar Cells. *Bulletin of advanced technology research*. 41-43.
- [6] J. Zhao, A. Wang, and M. A. Green, "24-5% Efficiency silicon PERT cells on MCZ substrates and 24-7% efficiency PERL cells on FZ substrates," *Progress in Photovoltaics: Research and Applications*, vol. 7, pp. 471-474, 1999.
- [7] G. SW, F. F, R. A, B. M, R. C, S. H, *et al.*, "The irresistible charm of a simple current flow pattern-25% with a solar cell featuring a full-area back contact," in *31st European Photovoltaic Solar Energy Conference*, Hamburg, Germany, 2015.
- [8] P. Campbell and M. Green, "Light trapping properties of pyramidally textured surfaces," *Journal of Applied Physics*, 1987.
- [9] T. Lauermaun, B. Frohlich, G. Hahn, and B. Terheiden, "Design considerations for industrial rear passivated solar cells," in *Photovoltaic Specialists Conference (PVSC), 2012 38th IEEE*, 2012, pp. 001710-001715.
- [10] J. Zhao, A. Wang, P. Campbell, and M. A. Green, "A 19.8% efficient honeycomb multicrystalline silicon solar cell with improved light trapping," *Electron Devices, IEEE Transactions on*, vol. 46, pp. 1978-1983, 1999.
- [11] C. Barugkin, Z. Ngwe-Soe, and K. R. Catchpole, "Photoluminescence enhancement towards high efficiency plasmonic solar cells," presented at the

- Photovoltaic Specialists Conference (PVSC), 2013 IEEE 39th, 2013.
- [12] R. Brendel, "Simple prism pyramids: a new light trapping texture for silicon solar cells," presented at the Photovoltaic Specialists Conference, 1993., Conference Record of the Twenty Third IEEE, 1993.
- [13] J. E. Cotter, "Optical intensity of light in layers of silicon with rear diffuse reflectors," *Journal of Applied Physics*, vol. 84, pp. 618-624, 1998.
- [14] M. v. Lare, F. Lenzmann, and A. Polman, "Dielectric back scattering patterns for light trapping in thin-film Si solar cells," *Optics Express*, 2013.
- [15] J. Haynos, J. Allison, R. Arndt, and L. Meulenber, "The COMSAT non-reflective silicon solar cell: A Second Generation Improved Cell," presented at the International Conference on Photovoltaic Power Generation, Hamberg, 1974.
- [16] A. Stesmans and V. V. Afanas'ev, "Thermally induced interface degradation in (100) and (111) Si/SiO<sub>2</sub> analyzed by electron spin resonance," *Journal of Vacuum Science & Technology B*, vol. 16, pp. 3108-3111, 1998.
- [17] P. J. Cousins and J. E. Cotter, "Minimizing lifetime degradation associated with thermal oxidation of upright randomly textured silicon surfaces," *Solar Energy Materials and Solar Cells*, vol. 90, pp. 228-240, 1/23/2006.
- [18] E. Franklin, K. Fong, K. McIntosh, A. Fell, A. Blakers, T. Kho, *et al.*, "Design, fabrication and characterisation of a 24.4% efficient interdigitated back contact solar cell," *Progress in Photovoltaics: Research and Applications*, pp. n/a-n/a, 2014.
- [19] B. Hoex, J. Schmidt, R. Bock, P. P. Altermatt, M. C. M. van de Sanden, and W. M. M. Kessels, "Excellent passivation of highly doped p-type Si surfaces by the negative-charge-dielectric Al<sub>2</sub>O<sub>3</sub>," *Applied Physics Letters*, vol. 91, p. 112107, 2007.
- [20] W. Liang, "Properties of Al<sub>2</sub>O<sub>3</sub> Films Deposited by Atomic Layer Deposition for Photovoltaic Applications," PhD, Australian National University, 2014.
- [21] L. E. Black and K. R. McIntosh, "Surface passivation of c-Si by atmospheric pressure chemical vapor deposition of Al<sub>2</sub>O<sub>3</sub>," *Applied Physics Letters*, vol. 100, p. 202107, 2012.
- [22] W. Yimao, K. R. McIntosh, A. F. Thomson, and A. Cuevas, "Low Surface Recombination Velocity by Low-Absorption Silicon Nitride on c-Si," *Photovoltaics, IEEE Journal of*, vol. 3, pp. 554-559, 2013.
- [23] J. Yota, "Effects of Deposition Method of PECVD Silicon Nitride as MIM Capacitor Dielectric for GaAs HBT Technology " in *Symposium on Silicon Nitride, Silicon Dioxide, and Emerging Dielectrics of the 2011 Electrochemical Society (ECS) Meeting*, Montreal, Canada, 2011.
- [24] D. Smith, "Review of Back Contact Silicon Solar Cells for low-cost Applications," O. o. S. a. T. Information, Ed., ed, 1999.
- [25] C. E. Chan, B. J. Hallam, and S. R. Wenham, "Simplified Interdigitated Back Contact Solar Cells," *Energy Procedia*, vol. 27, pp. 543-548, // 2012.
- [26] J. B. Heng, F. Jianming, B. Kong, C. Yongkee, W. Wei, X. Zhigang, *et al.*, "High-Efficiency Tunnel Oxide Junction Bifacial Solar Cell With Electroplated Cu Gridlines," *Photovoltaics, IEEE Journal of*, vol. 5, pp. 82-86, 2015.
- [27] T. Koschwitz, B. Meinel, and J. Acker, "Application of Confocal Microscopy to Evaluate the Morphology of Acidic Etched Mc-silicon," *Energy Procedia*, vol. 38, pp. 234-242, // 2013.
- [28] P. B. C.-. [http://www.brewerscience.com/uploads/products/protek/datasheets/ds\\_protek\\_b3.pdf](http://www.brewerscience.com/uploads/products/protek/datasheets/ds_protek_b3.pdf).
- [29] D. E. Kane and R. M. Swanson, "Measurement of the emitter saturation current by a contactless photoconductivity decay method," in *18th IEEE Photovoltaic Specialist Conference*, Las Vegas, 1985, pp. 578-583.
- [30] E. Daub and P. Würfel, "Ultralow Values of the Absorption Coefficient of Si Obtained from Luminescence," *Physical Review Letters*, vol. 74, pp. 1020-1023, 02/06/ 1995.
- [31] P. Lighthouse. Available: [www.pvlighthouse.com.au](http://www.pvlighthouse.com.au)
- [32] N. Zin, Andrew Blakers, Keith McIntosh, Evan Franklin, Teng Kho, Johnson Wong, Thomas Mueller, Armin G. Aberle, Zhiqiang Feng, Qiang Huang, "19% Efficient N-Type All-Back-Contact Silicon Wafer Solar Cells With Planar Front Surface," in *Australian Solar Energy Society Conference*, Sydney, Australia, 2011.